

Standard model for liquid water withstands x-ray probe

David Prendergast* and Giulia Galli†

Lawrence Livermore National Laboratory, L-415, P.O. Box 808, Livermore, CA 94551.

(Dated: November 7, 2018)

We present a series of ab-initio calculations of spectroscopic properties of liquid water at ambient conditions. Our results show that all available theoretical and experimental evidence is consistent with the standard model of the liquid as comprising molecules with approximately four hydrogen bonds. In particular, this model cannot be discounted on the basis of comparisons between measured and computed x-ray absorption spectra (XAS), as recently suggested. Our simulations of ice XAS including the lowest lying excitonic state are in excellent agreement with experiment and those of the TIP4P model of water are in reasonable agreement with recent measurements. Hence we propose that the standard, quasi-tetrahedral model of water, although approximate, represents a reasonably accurate description of the local structure of the liquid.

PACS numbers: 61.10.Ht, 78.70.Dm, 61.20.Ja, 61.20.Gy

Understanding the hydrogen-bonding in liquid water is fundamental to a thorough comprehension of the driving forces behind many physical, chemical and biological processes. For the past forty years, water has been modeled as having a local structure not dissimilar to that of the solid phase. In crystalline ice, each molecule is hydrogen-bonded to exactly four others, in an approximately tetrahedral arrangement.^{1,2} In the standard model of the liquid the local, molecular coordination is also approximately tetrahedral, with about 3.6 hydrogen bonds/molecule.³ Classical potentials, fitted to x-ray and neutron scattering data and to measured thermodynamic properties, yield a quasi-tetrahedral local structure of the liquid when used in molecular dynamics (MD) simulations, and simultaneously reproduce many other physical properties.⁴ More recently, first principles, density functional theory^{5,6} (DFT) calculations have confirmed the quasi tetrahedral coordination of water molecules in the liquid. However, when neglecting proton quantum effects, converged DFT-MD simulations produce a more ice-like structure for the liquid^{7,8} than that inferred from experimental estimates of the radial distribution functions.³

X-ray absorption spectroscopy techniques may help to elucidate the local structure of liquid water. In these approaches, high-energy, x-ray photons excite electrons from deep atomic core levels to states above the Fermi level. If structural models are available, together with their electronic structure, it is possible to simulate the x-ray absorption spectra (XAS) of several candidate structures and establish which one best represent the measurements. The success of this approach hinges on the accuracy of XAS simulations and that is the focus of this letter.

Recent XAS experiments on water have questioned the standard, tetrahedral model of the liquid.⁹ These experi-

ments have compared the XAS of bulk ice, the ice surface and water and concluded that the liquid contains significantly more broken hydrogen-bonds than previously thought. The spectra are qualitatively consistent with independent experiments,^{10,11} however, their interpretation remains controversial. In conjunction with DFT calculations of the XAS, the experimental results have led to the proposal of a new structural model in which each molecule is strongly hydrogen-bonded to only two others. These conclusions have major implications for the physics and chemistry of liquid water.

In this work, we report on first principles DFT simulations of the XAS of ice and liquid water at ambient pressures. Our approach can reliably predict the near K edge structure of oxygen in crystalline ice. Given the very good agreement between theory and experiment found in the case of ice, we used the same approach to simulate the XAS of the liquid as described by the TIP4P classical potential;⁴ this potential yields a local structure consistent with the standard model. Our results are in reasonable agreement with experimental XAS. Further analysis of molecular species of the liquid with broken hydrogen-bonds shows that their spectral signature is qualitatively different from the average XAS of the liquid; hence increasing the proportion of these species would yield spectra which are significantly different from the measured ones. We also discuss previous theoretical approaches to simulate the XAS of water,^{9,12} and we show that our results and those present in the literature are all consistent with a quasi-tetrahedral model of the local structure of the liquid.

The x-ray absorption cross section is calculated to first order using Fermi's golden rule:

$$\sigma(\omega) = 4\pi^2\alpha_0\hbar\omega \sum_f |M_{i\rightarrow f}|^2 \delta(E_f - E_i - \hbar\omega), \quad (1)$$

where $\hbar\omega$ is the energy of the absorbed photon, which should match the energy difference $E_f - E_i$ between initial and final electronic states; α_0 is the fine structure constant; and $M_{i\rightarrow f}$ are the matrix elements of the transition between initial and final states: $|\Psi_i\rangle$ and $|\Psi_f\rangle$,

*Present address: University of California, Berkeley

†Present address: University of California, Davis

evaluated within the electric-dipole approximation as

$$M_{i \rightarrow f} = \langle \Psi_f | \hat{\epsilon} \cdot \mathbf{R} | \Psi_i \rangle \approx S \langle \psi_f | \hat{\epsilon} \cdot \mathbf{r} | \psi_i \rangle, \quad (2)$$

where $\hat{\epsilon}$ is the polarization direction of the electromagnetic vector potential, \mathbf{R} and \mathbf{r} are the many-electron and single-electron position operators respectively, and $|\psi_{i,f}\rangle$ refer to the pair of single-particle states involved in the transition. Here the initial state is fixed as the $1s$ eigenstate of the oxygen atom. Single-particle approximations of the many-electron matrix elements are accurate up to a factor S , approximately constant for all transitions.¹³

In our approach the final state of the electronic system is calculated in the presence of the core hole which results from the x-ray excitation. To reduce the computational cost, we occupy only the first available empty band with the excited electron and relax the DFT electronic structure within this constraint.¹⁴ We then use the corresponding self-consistent potential to generate unoccupied levels higher in energy than the first excitation. We use the pseudopotential approximation, and model the x-ray excited atom with a pseudopotential derived from an oxygen atom with one electron removed from the $1s$ level. We employ norm-conserving Hamann pseudopotentials¹⁵ for oxygen and a Gaussian pseudopotential for hydrogen by Giannozzi. The breaking of spin-degeneracy accompanying a single-electron excitation is not included. The matrix elements $M_{i \rightarrow f}$ between the atomic core level and the excited conduction band are computed using a frozen-core approximation.^{12,16,17} We employ DFT within the generalized-gradient-approximation using the Perdew-Burke-Ernzerhof exchange-correlation functional (PBE-GGA)¹⁸ and the PWSCF code.¹⁹ The single particle wavefunctions are expanded in a plane-wave basis with an energy cut-off of 85 Ryd.

Recent NEXAFS experiments^{9,20} reported x-ray absorption of crystalline ice samples prepared by molecular deposition on the Pt[111] surface. Helium scattering indicates²¹ the presence of molecular crystals with surfaces consistent with either the (0001) surface of hexagonal ice (*Ih*) or the (111) surface of cubic ice (*Ic*). (Recent work²² indicates that coverage of crystalline ice on Pt[111] may not be uniform). In Fig 1 we compare the NEXAFS measurements with our calculated XAS.

We used lattice constants of ice *Ih* yielding a density of 1.00 g cm^{-3} with a c/a ratio of 0.945. The density of ice *Ic* was fixed at the experimental value of 0.931 g cm^{-3} using $c/a = 1.0$.²⁹ The primitive cell atomic structures were relaxed, with these constraints on the unit cell volumes, until the forces computed using PBE-GGA were less than 10^{-3} a.u.

The primitive cell of ice *Ih* (*Ic*) contains 12 (8) water molecules and we constructed a $2 \times 2 \times 2$ supercell of 96 (64) molecules for our calculations.³⁰ The excited state electronic structure, including the excited electron in the lowest available conduction band, was converged using a uniform grid of 27 (64) k -points in the Brillouin zone containing 10 (36) symmetry-inequivalent points. All absorption cross sections were averaged over the three

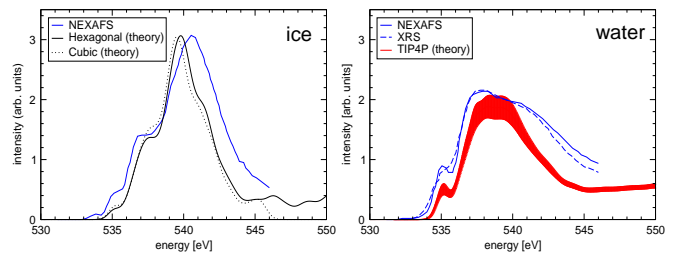


FIG. 1: *Left*: NEXAFS spectrum of crystalline ice I from Ref.⁹ (blue) and calculated XAS of hexagonal ice *Ih* (black, solid) and cubic ice *Ic* (black, dotted). *Right*: NEXAFS (blue, solid) and XRS (blue, dashed) spectra of water from Ref.⁹, and calculated XAS of water (red) from the TIP4P MD simulation at 300 K. Vertical thickness of the calculated curve is the associated standard error from a sample of 32 water molecules.

Cartesian directions.

The agreement between calculated and measured XAS (see Fig. 1) is excellent, with all qualitative features reproduced accurately. The computed spectrum is aligned with an onset energy of 535 eV associated with the lowest computed transition (at the zone center), broadened using a Gaussian lineshape with 0.4 eV standard deviation, and renormalized to reproduce the peak height of experiment. In general the width of the computed peaks is too narrow in comparison with experiment. This is consistent with the general underestimation of band-width within current local approximations to DFT and originates from an approximate description of exchange interactions. Improvements are possible using self-interaction corrected DFT calculations²³ or by using *GW* quasi-particle corrections.²⁴ Note that ice *Ih* and *Ic* differ structurally only beyond first nearest neighbor molecules. Consequently, their spectra are very similar, given the short spatial range of the oxygen K edge transition probability, which is proportional to the overlap of the p -character of conduction bands with the oxygen $1s$ -orbital, possessing a 0.2 \AA effective radius.

We model liquid water using the classical, TIP4P point charge model,⁴ which qualitatively reproduces the phase diagram of water,²⁵ and which we have previously used to analyze the electronic structure of the liquid.²⁶ In this model water molecules are treated as rigid. We took 10 snapshots of 32 water molecules from a 200 ps MD simulation^{27,28} spaced 20 ps apart. To approximate the XAS experiment, we average computed spectra from each molecule in a given snapshot and further average over all snapshots. In total we combined the results of 320 spectral calculations to approximate the XAS of the liquid. We found very little variation between the XAS of individual, uncorrelated snapshots computed using only the zone-center k -point. Therefore, we picked one representative snapshot of 32 molecules, and carried out calculations using 27 k -points in the Brillouin Zone, for each excited molecule. Each spectrum of discrete transitions is broadened with a Gaussian lineshape with a standard

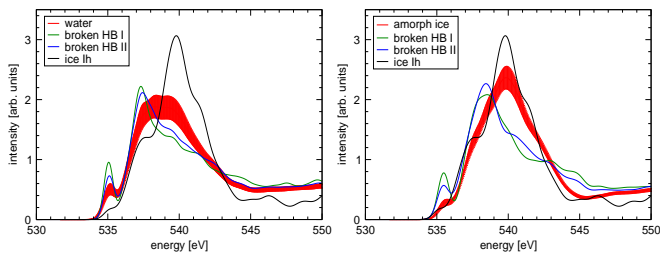


FIG. 2: *Left* : Comparison of the calculated XAS of water (red) and crystalline ice *Ih* (black). *Right*: A similar comparison between ice *Ih* and a model of amorphous ice (red). Also indicated in both panels are the characteristic spectra from water molecules with at least one broken donor hydrogen bond (see text). Vertical thickness indicates standard error as in Fig. 1. We assume that the experimental data for solid and liquid⁹ are quantitatively comparable and use the same normalization factor and onset energy for both theoretical curves.

deviation of 0.3 eV. The averaged XAS is compared in Fig. 1 with the experimental NEXAFS and XRS spectra of water at 300 K.⁹ The vertical width of the theoretical curve indicates an estimate of the standard error at a given energy. Our calculation is in good qualitative agreement with experiment, indicating that the tetrahedral local model of the liquid accounts reasonably well for measured XAS.

The contribution to the XAS of the liquid from molecules with broken or distorted hydrogen-bonds (HB) is compared to that of the entire liquid in Fig. 2. Our model contains approximately 20% of molecules with broken HB, which are defined according to two definitions: (I) exceeding a maximum separation of oxygen atoms of 3.5 Å and a maximum angle of the donated hydrogen from the line joining both oxygens of 40°; (II) exceeding a maximum oxygen-oxygen separation which depends on the angle as outlined in Ref.⁹.

There is a clear, qualitative difference between the spectra of species with broken HB and the averaged spectrum. Such differences were predicted in Ref.⁹, where it was concluded that the liquid should contain about 80% of broken HB species in order to produce the measured XAS. We do not find this to be necessary when using our approach for the calculation of XAS, which differs from that used in Ref.⁹.

In Fig. 2 we also compare the XAS of ice *Ih* and of a rather primitive model of amorphous or disordered ice, generated using the TIP4P potential by quenching a 300 K liquid sample of 32 molecules down to 100 K. One snapshot at this temperature was used to generate the XAS in Fig. 2. The spectra of the broken HB species are qualitatively similar in the disordered sample and in the liquid. However, only one (two) of the molecules in this snapshot had less than two donor HB according to definition I (II), and yet the XAS is qualitatively different from that of the crystalline sample. Clearly disorder plays a role in reducing the peak height at 539–540 eV.

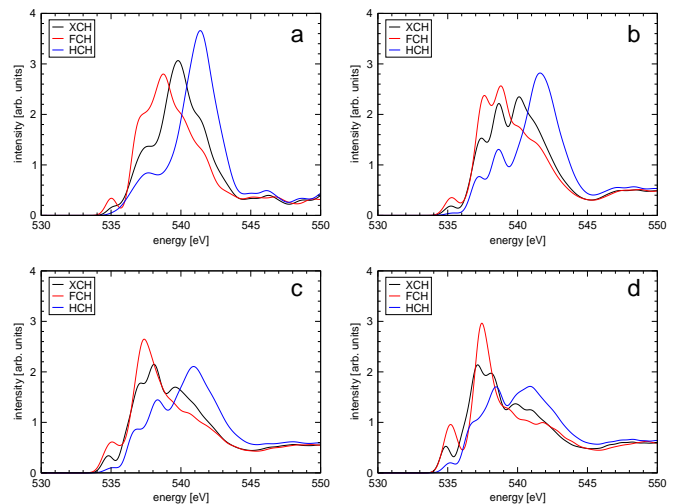


FIG. 3: Comparison of DFT XAS within various approximations for the x-ray absorption process, *viz.* excited state core hole (XCH), full core hole (FCH) and half core hole (HCH). (a) hexagonal ice; (b) amorphous ice; (c) liquid water; (d) liquid water sampling only broken-hydrogen-bonded species. Note that the calculated HCH spectrum of a standard, quasi-tetrahedral liquid water model appears ice-like in comparison with experiment, however it is still clearly distinguishable from ice XAS.

We also observe an increase in intensity around 538 eV and at much higher energies above 545 eV. Both of these trends are seen in the liquid as well, and can be associated with disorder in the oxygen sublattice. On the other hand, the significant increases in intensity at the onset (535 eV) and the main-edge (537–538 eV) found in the liquid can be associated with broken HB, of which there are approximately 4–6 times as many in the liquid sample. There are therefore two important effects accounting for the difference between XAS of ice and XAS of the liquid: broken HB and disorder of the oxygen sublattice.

In the recent literature, two approaches have been applied to the simulation of the XAS of water in various phases: the full core hole (FCH) and half-core hole (HCH) approaches. The FCH technique¹² is analogous to the one adopted here, except that there is no self-consistent inclusion of the excited electron. Such an approach should accurately reproduce the higher energy excitations to progressively more delocalized states, and at high energy yield the same results as our approach, which we call excited-state-core-hole (XCH). However, accounting for the impact of a localized excited electron at low energies leads to differences between FCH and XCH results; these are shown in Fig. 3. FCH tends to overestimate the absorption cross section at and near the onset, consequently underestimating the main peak height, by virtue of the oscillator strength sum-rule.

In the HCH approach only half of an electron is removed from the core-state, thereby simulating a transition state in the x-ray excitation process. We have found that in the presence of the HCH pseudopotential, inclu-

sion of an excited electron at the conduction band minimum has almost no impact on the calculated XAS. The HCH spectra tend to overemphasize the main peak and underestimate the excitonic near-edge intensity. This is consistent with the reduced binding energy of the half-core-hole in the excited oxygen atom.

We note that the same spectral trends exist in all approaches (FCH, XCH and HCH) with respect to increasing disorder and number of broken HB: a decrease in the main peak height and an increase in intensity at the near-edge are observed. However, in the limit of converged k -point sampling and when employing homogeneous numerical broadenings, we find that only the XCH approach provides a consistent agreement with experiment.

In summary, using DFT electronic structure calculations, we find excellent agreement between the calculated and experimentally measured XAS of ice. Using the TIP4P classical potential to simulate a standard, quasi-tetrahedral model of liquid water we find reasonable agreement between our DFT calculations and experiment. Furthermore, restriction of our analysis to those

molecular species with broken HB leads to simulated XAS which are qualitatively different from experiment. Therefore we conclude that the percentage of broken HB in the standard model is consistent with experimental observations. Finally, despite the different spectra produced by various approximations used to simulate the x-ray absorption process, we find no conclusive evidence within each approach to discount the standard model of the liquid.

Acknowledgments

We wish to acknowledge E. Schwegler, T. Ogitsu, G. Cicero, F. Gygi, and A. Correa for useful discussions. This work was performed under the auspices of the U.S. Department of Energy at the University of California/Lawrence Livermore National Laboratory under Contract No. W-7405-Eng-48.

-
- ¹ J. D. Bernal and R. H. Fowler, *J. Chem. Phys.* **1**, 515 (1933).
- ² L. Pauling, *J. Am. Chem. Soc.* **57**, 2680 (1935).
- ³ A. K. Soper, *Chem. Phys.* **258**, 121 (2000).
- ⁴ W. L. Jorgensen, J. Chandrasekhar, J. D. Madura, R. W. Impey, and M. L. Klein, *J. Chem. Phys.* **79**, 926 (1983).
- ⁵ P. Hohenberg and W. Kohn, *Phys. Rev.* **136**, B864 (1964).
- ⁶ W. Kohn and L. J. Sham, *Phys. Rev.* **140**, A1133 (1965).
- ⁷ J. C. Grossman, E. Schwegler, E. W. Draeger, F. Gygi, and G. Galli, *J. Chem. Phys.* **120**, 300 (2004).
- ⁸ E. Schwegler, J. C. Grossman, F. Gygi, and G. Galli, *J. Chem. Phys.* **121**, 5400 (2004).
- ⁹ P. Wernet, D. Nordlund, U. Bergmann, M. Cavalleri, M. Odellius, H. Ogasawara, L. A. Näslund, T. K. Hirsch, L. Ojamäe, P. Glatzel, et al., *Science* **304**, 995 (2004).
- ¹⁰ H. Bluhm, D. F. Ogletree, C. S. Fadley, Z. Hussain, and M. Salmeron, *J. Phys.: Condens. Matter* **14**, L227 (2002).
- ¹¹ J. D. Smith, C. D. Cappa, K. R. Wilson, B. M. Messer, R. C. Cohen, and R. J. Saykally, *Science* **306**, 851 (2004).
- ¹² B. Hetényi, F. D. Angelis, P. Giannozzi, and R. Car, *J. Chem. Phys.* **120**, 8632 (2004).
- ¹³ G. D. Mahan, *Many particle physics* (Kluwer Academic/Plenum, New York, 2000), 3rd ed., (Physics of Solids and Liquids).
- ¹⁴ S.-D. Mo and W. Y. Ching, *Phys. Rev. B* **62**, 7901 (2000).
- ¹⁵ D. R. Hamann, *Phys. Rev. B* **40**, 2980 (1989).
- ¹⁶ M. Taillefumier, D. Cabaret, A.-M. Flank, and F. Mauri, *Phys. Rev. B* **66**, 195107 (2002).
- ¹⁷ P. E. Blöchl, *Phys. Rev. B* **50**, 17953 (1994).
- ¹⁸ J. P. Perdew, K. Burke, and M. Ernzerhof, *Phys. Rev. Lett.* **77**, 3865 (1996).
- ¹⁹ S. Baroni, A. D. Corso, S. de Gironcoli, and P. Giannozzi, URL <http://www.pwscf.org>.
- ²⁰ S. Myneni, Y. Luo, L. A. Näslund, M. Cavalleri, L. Ojamäe, H. Ogasawara, A. Pelmenchikov, P. Wernet, P. Väterlein, C. Heske, et al., *J. Phys.: Cond. Matter* **14**, L213 (2002).
- ²¹ J. Braun, A. Glebov, A. P. Graham, A. Menzel, and J. P. Toennies, *Phys. Rev. Lett.* **80**, 2638 (1998).
- ²² G. A. Kimmel, N. G. Petrik, Z. Dohnálek, and B. D. Kay, *Phys. Rev. Lett.* **95**, 166102 (2005).
- ²³ J. P. Perdew and A. Zunger, *Phys. Rev. B* **23**, 5048 (1981).
- ²⁴ M. S. Hybertsen and S. G. Louie, *Phys. Rev. B* **34**, 5390 (1986).
- ²⁵ E. Sanz, C. Vega, J. L. F. Abascal, and L. G. MacDowell, *Phys. Rev. Lett.* **92**, 255701 (2004).
- ²⁶ D. Prendergast, J. C. Grossman, and G. Galli, *J. Chem. Phys.* **123**, 014501 (2005).
- ²⁷ H. J. C. Berendsen, D. van der Spoel, and R. van Drunen, *Comp. Phys. Comm.* **91**, 43 (1995).
- ²⁸ E. Lindahl, B. Hess, and D. van der Spoel, *J. Mol. Mod.* **7**, 306 (2001).
- ²⁹ The density dependence of the qualitative XAS of ice was not noticeable within this 7% range. However, a full exploration of the structural phase space was not carried out in this investigation.
- ³⁰ Using a single k -point at the zone-center we found no significant spectral difference in XAS computed using $2 \times 2 \times 2$ or $3 \times 3 \times 3$ supercells for ice *Ih*.